Hydrothermal Gasification Performance of Iranian Rice Straw in Supercritical Water Media for Hydrogen-Rich Gas Production

Mohammad Salimi,*[,a] Behnam Nejati, [a] Ali Karimi, [b] and Ahmad Tavasoli [a]

As a clean and green alternative fuel to replace fossil fuels, hydrogen could be an ideal fuel for the future. Supercritical water gasification of lignocellulosic agricultural residues results in H_2 production with zero CO_2 emission, which makes this technique an attractive technology for hydrogen generation from biomass. Structural analyses were performed to determine the lignin, cellulose, and hemicellulose contents in feedstock. The effects of different process variables (temperature, reaction time, and feed concentration) on supercritical water gasification of Iranian rice straw (IRS) were evaluated. IRS, which has a high content of cellulose and hemicellulose, has significant potential for gaseous product generation under the supercritical water condition. The maximum H_2 production of 5.56 mmol/gr of biomass was achieved at 440 °C (temperature), 20 min (reaction time), and 2 wt. % (feed concentration).

Keywords: Agricultural residue; Gasification; Hydrogen; Supercritical water

Contact information: a: School of Chemistry, College of Science, University of Tehran, Tehran, Iran; Phone: (98)-21-61113643; b: Research Institute of Petroleum Industry, Tehran, Iran;
** Corresponding author: salimi.m@ut.ac.ir*

INTRODUCTION

Fossil fuels, which have emerged under relatively high temperatures and pressures over millions of years underground, are limited in supply as non-renewable resources. To limit greenhouse gas emissions originating from fossil fuel consumption, renewable resources are gaining attention in most parts of the world. Renewable energy sources can reduce the rate of global warming and concerns about the supplementary fuel reserves. Using renewable energy resources to maximize energy efficiency and improve energy conservation requires novel methods that are suitable for achieving energy security and sustainable energy development (Hiremath *et al.* 2009). Hydrogen has high energy efficiency and is environmentally friendly, and it is an ideal fuel for the future.

According to Texas Renewable Energy Industries Association's (TERIA) definition (Anon 2014), renewable energy includes all energy sources that regenerate themselves naturally in a short period of time. Due to this definition, renewable energy cannot originate from fossil or mineral resources. Biomass is a great renewable energy resource that has attracted global interest (Barati *et al.* 2014). Biomass is an organic substance mainly composed of carbon, hydrogen, and oxygen, which is living or has lived recently. This useful raw material stores solar energy in its molecular bonds and has high potential as a renewable energy resource (Tavasoli *et al.* 2015). Examples of biomass include plants (trees, algae, corn, wheat, and grass), fruit, vegetable wastes, plant-based waste (rice straw, canola stalk, *etc.*), urban waste, and agro-industrial waste (Tekin *et al.* 2014). Hydrogen gas as a fuel provides zero carbon emissions. Biomass-derived hydrogen

is a clean, renewable energy source that could preserve the environment and improve energy security (Rashidi and Tavasoli 2014). It is an environmentally friendly fuel with high energy capacity and a low heating value (LHV), which is 2.4, 2.8, and 4 times greater than that of methane, gasoline, and coal, respectively. It produces only water as a by-product of combustion.

A biomass is any heterogeneous mixture of organic substances and a small amount of inorganic substances. Cellulose, hemicellulose, lignin, and extractives are the main components of lignocellulosic materials. Figure 1 provides a schematic illustration of a plant cell wall from lignocellulosic biomass.

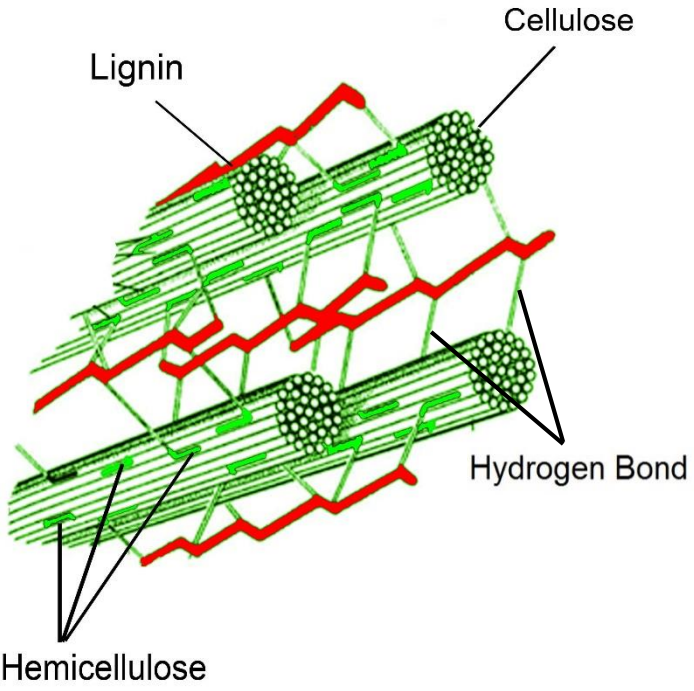

Fig. 1. Plant cell wall of lignocellulosic biomass. Thin green lines represent hydrogen bonds which connect lignin to polysacharide structure

Cellulose

Cellulose is the most abundant organic material on earth, with an annual production of over 50 billion tons. It is a skeletal polysaccharide with a glucose monomer unit and β-1,4 glycoside linkages (Mohan *et al.* 2006). The basic repeating unit of the cellulose polymer consists of two glucose anhydride units, called a cellobiose unit. Cellulose is a condensation polymer of glucose, similar to starch, but the links between the glucose monomers are slightly different. It is insoluble in water because of its low-surface-area crystalline form, which is held together by hydrogen bonds. The degree of crystallinity of cellulose varies with its origin and treatment (Huber and Dumesic 2006).

Hemicellulose

Compared with cellulose, hemicellulose consists of various polymerized monosaccharides including five carbon sugars (usually xylose and arabinose), six-carbon sugars (galactose, glucose, and mannose), and 4-O-methyl glucuronic acid and galacturonic acid residues. It exists in association with cellulose in the cell wall (Huber

and Dumesic 2006; Mohan *et al*. 2006). Because of its structure and branched nature, hemicellulose is amorphous and relatively easy to hydrolyze to its monomer sugars.

Lignin

Lignin is a three-dimensional, highly branched, polyphenolic substance that consists of an irregular array of variously bonded hydroxyl- and methoxy-substituted phenyl propane units (Bridgewater 2004). As a necessary component for the plant to be classified as woody, lignin is an amorphous cross-linked resin, serving as a cement between the wood fibers and a stiffening agent within the fibers. Lignin is often associated with the cellulose and hemicellulose materials making up lignocellulose compounds; these materials must be broken down to make the cellulose or hemicellulose accessible to hydrolysis (Huber and Dumesic 2006). Lignin has an amorphous structure, which leads to a large number of possible inter-linkages between individual units. Ether bonds predominate between lignin units, unlike the acetal functions found in cellulose and hemicellulose. Covalent linking also exists between lignin and polysaccharides, which strongly enhances the adhesive bond strength between cellulose fibers and its lignin "potting matrix" (Jacobs-Young *et al*. 1998).

Lignocellulosic biomasses can be converted into hydrogen *via* different technologies, primarily thermochemical (pyrolysis, gasification, supercritical water gasification) or biochemical conversion. Due to the use of water as a reaction medium, supercritical water gasification (SCWG) has several advantages compared with other methods.

The dielectric constant of supercritical water (temperatures and pressures above 374 °C and 22.1 MPa, respectively) decreases very strongly, and it behaves as a non-polar solvent. All gases and most organic substances dissolve completely in supercritical water, which makes the reaction media homogeneous. This homogeneous environment decreases the mass transfer resistance as biomass dissolves in supercritical water. This effect enables a quick and almost complete hydrothermal gasification of biomass into gaseous products with minimum char formation (Huang and Ramaswamy 2011; Kean *et al.* 2013).

The mechanism of biomass gasification in supercritical water has been studied, but biomass conversion in this media is complicated and hard to explain (Susanti *et al.* 2012). Despite these difficulties, this process can be summarized in the three main reactions of steam gasification (1), water-gas shift (2), and methanation (3), as follows:

$$C_xH_yO_z + (1\text{-}y)\ H_2O \rightarrow xCO_2 + (x/2+1\text{-}y)\ H_2 \quad (1)$$

$$CO + H_2O \leftrightarrow CO_2 + H_2 \quad (2)$$

$$CO + 3H_2 \leftrightarrow CH_4 + H_2O \quad (3)$$

In the hydrolysis reaction, biomass decomposes into intermediate compounds (*e.g*., glucose, fructose) (Hao 2003; Yu *et al.* 2014). These intermediate compounds further decompose to gaseous products such as hydrogen (H_2) and carbon dioxide (CO_2), with small amounts of methane (CH_4) and carbon monoxide (CO). To increase hydrogen production, the water-gas shift reaction must be enhanced, and the methanation reaction must be inhibited. Thus, high-temperature water can enhance hydrogen production.

Biomass degradation and subsequent gasification in supercritical water depends on its structure, which varies in different resources (Fig. 2). Lignocellulosic materials in

agricultural wastes can be used for hydrogen production in supercritical water. Due to their abundance and accessibility, these materials have great potential for energy generation.

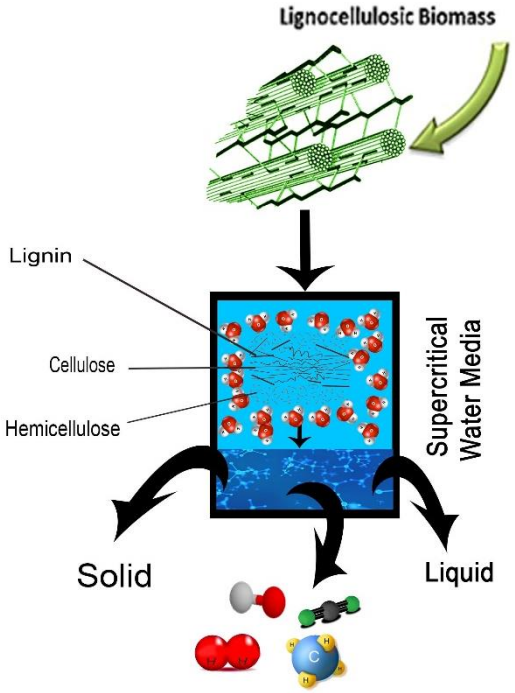

Fig. 2. Supercritical water gasification of lignocellulosic biomass

Iran is able to produce 8.78 million tons (MT) of energy from agricultural wastes annually. Although over 33% of Iranian territory is appropriate for the cultivation of agricultural products, limited water resources only makes cultivation possible in 12% of this area. About 7% of Iran is devoted to the Alborz forest in the north and the Zagros forest in the west, which produce forest wastes that could be converted into renewable fuels. Mazandaran province with 30 MT annual production of rice has a great potential for energy generation by processing this agricultural waste. Iranian rice straw (IRS) contains enough cellulose and hemicellulose to be considered as biomass source for gasification.

This study focused on the production of hydrogen gas due to its clean and efficient nature as an energy source. The effect of process variables on the lignocellulosic biomass gasification in supercritical water media for hydrogen production were investigated, and the process variables were optimized for further studies.

EXPERIMENTAL

Materials

The biomass particles used for the experiments were supplied from agriculture farms around Sari, located in Mazandaran province, Iran. Taking into account the statistics of agricultural products of this province, rice straw was selected as the most abundant feedstock. Pretreatment for feedstock included washing, drying, grinding, and sieving to achieve clean and dry biomass particles with dimensions up to 150 µm. Elemental analyses

of biomass samples were conducted using a CHNS analyzer (Vario EL III, Elementar, Frankfurt, Germany).

Experimental setup

A schematic of the experimental setup is shown in Fig. 3. The set-up contained a batch micro reactor made of 316 stainless steel tubes with total volume of 26 mL. A total of 0.15 g of feedstock was added to 6 g of deionized water to obtain a 2.5 wt.% mixture. The mixture was injected into the reactor using a syringe. Argon as an inert gas stream was used for vacating the reactor and removing air for 4 min and flow rate 60 mL/min. Also the reactor was then pressurized with this gas up to 10 bars to avoid vaporization of water during heating, and it was plunged in a molten salt bath that contains a mixture of potassium nitrate, sodium nitrate, and sodium nitrite. The molten salt bath temperature was measured using a K-type thermocouple and was maintained in 440 °C using a PID temperature controller. When the reactor was fully sealed and pressurized to 10 bar, the salt bath temperature leads to an increase in pressure which is corresponded to equilibrium pressure of water at the given temperature.

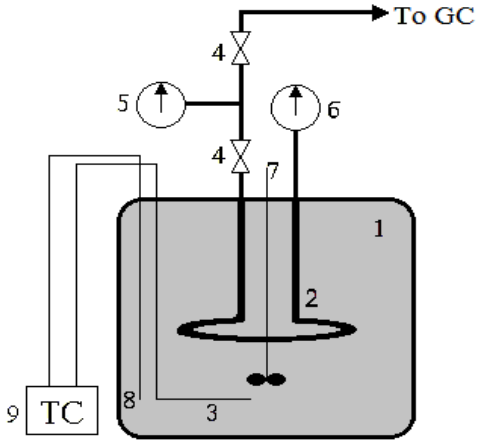

Fig. 3. Schematic of the batch micro reactor system: 1) molten salt bath, 2) tubular batch reactor, 3) electrical heater, 4) high pressure valves, 5) low-pressure gauge, 6) high pressure gauge, 7) mixer, 8) k-type thermocouple, 9) temperature controller

After a given reaction time, the reactor was removed from the molten salt bath and plunged in a water bath for rapid cooling to room temperature. The final pressure was measured using a low pressure gage to calculate the produced gas. The remaining products in the reactor were washed with water and filtered to separate solid residue. All experiments were performed 3 times under the same experimental conditions, and the data reported are the averages of repetitive runs (Mehrani *et al.* 2015).

At the end of each experiment, the free volume, final pressure, and temperature of the reactor were used to calculate the total gas yield. The composition and amount of each component were measured using gas chromatographs (Varian 3400 and Teyfgostar-Compact, Tehran, Iran).

Cellulose, Hemicellulose, and Lignin Determination

Extractives

Extractives were measured according to TAPPI regulation (TAPPI T204 cm-97 (1997)). A mixture of acetone and ethanol (1:2) was used as the solvent. A total of 2 g of biomass (based on dry weight) were put in a thimble, and the complex was placed in a Soxhlet extractor. Then, 200 mL acetone and 100 mL alcohol were added to a 500-mL flask that was attached to the system. The system was set for 8 h on a heater in which its temperature was regulated to achieve flushing every 10 min. During this period, soluble extractives were transferred to the flask. After this time, the thimble was brought out from the Soxhlet extractor, and boiling of the bottom residue of the flask was continued to reduce the volume of solvent. At the end, the materials in the flask were poured into a beaker and transferred to an oven with constant temperature of 103 °C. After 24 h, the extracted sediment was weighed. The alcohol-acetone soluble extractives were determined by Eq. 4:

$$\%\ \text{Extractives} = \frac{\text{dry extractives weight that remains in ballon}}{\text{dry biomass weight}} \times 100 \quad (4)$$

Ash

Ash measurements were performed according to TAPPI regulation (TAPPI T211om-02(2002)). Briefly, 4 g of biomass (based on dry weight) was placed in a crucible, which was placed over a flame. The sample was burned until there was no more smoke, and the crucible was placed in an electric furnace at 575 °C for 3 h. Next, the crucible was placed in a desiccator for 45 min. The ash content was determined using the following equation:

$$\%\ \text{Ash} = \frac{\text{dry Ash weight that remains in coarse}}{\text{dry biomass weight}} \times 100 \quad (5)$$

Cellulose

Cellulose was measured by the nitric acid technique TAPPI (TAPPI T264cm-97 (1997)). According to this method, 2 g of biomass without any extractives (based on dry weight after the measurement of extractives) was placed in a 250-mL flask, and 100 mL of 96% ethanol and 50 mL of 65% nitric acid were added. The materials in the flask were heated to their boiling point for about 1 h. This solution was filtered by a coarse filter, and the resulting solution was returned to the flask. This action was repeated after adding the same amount of acid and alcohol. After the third time, the material in the flask was placed on coarse filter, and after precipitation, it was placed in an oven at 103 °C for 24 h to dry completely. The weight difference between these two modes determines the amount of cellulose, as calculated from the following equation:

$$\%\ \text{Cellulose} = \frac{\text{Cellulose dry weight}}{\text{dry biomass weight}} \times 100 \quad (6)$$

Lignin

Lignin was measured in accordance with the TAPPI regulation (TAPPI T222om-02 (2006)). For this purpose, 1 g of biomass without any extractives (based on dry weight) was added to a 50-mL beaker with 15 mL of 72% sulfuric acid, and the mixture was stirred for 2 h. During this operation, sulfuric acid solved biomass polysaccharides in itself. After 2 h, this mixture was poured on round-bottom flasks 1000 mL, and 560 mL of distilled

water was added. The flask was placed on the heater, and after installation of the condenser, the contents of the flask boiled for 4 h smoothly. During this period, carbohydrates in the biomass dissolved completely, and lignin remained as an insoluble precipitate. At the end of 4 h, the solution inside the flask was filtered by the Buchner vacuum system and washed with distilled water to remove the remaining acid. The Buchner filter and its contents were placed in an oven at 103 °C for approximately 24 h. The amount of lignin and its percentage was calculated from the following equation:

$$\% \text{ Lignin } = \frac{\text{Lignin dry weight}}{\text{dry biomass weight}} \times 100 \quad (7)$$

Hemicellulose

Finally, the hemicellulose was calculated through the following equation:

$$\% \text{ Hemicellulose } = 100 - [\%\text{Cellulose} + \%\text{Ash} + \%\text{Lignin} + \%\text{Extractives}] \quad (8)$$

Methods

Figure 4 shows the most important properties of water in the supercritical region (*e.g.*, dielectric constant, hydrocarbon solubility, density, *etc*.). The temperature ranged from 400 to 440 °C and was a process variable. As shown in Fig. 5, at a constant quantity of water and biomass, the pressure reached 260 bars when the temperature reached 440 °C. Therefore, 440 °C was selected as the maximum allowable temperature for safety purposes.

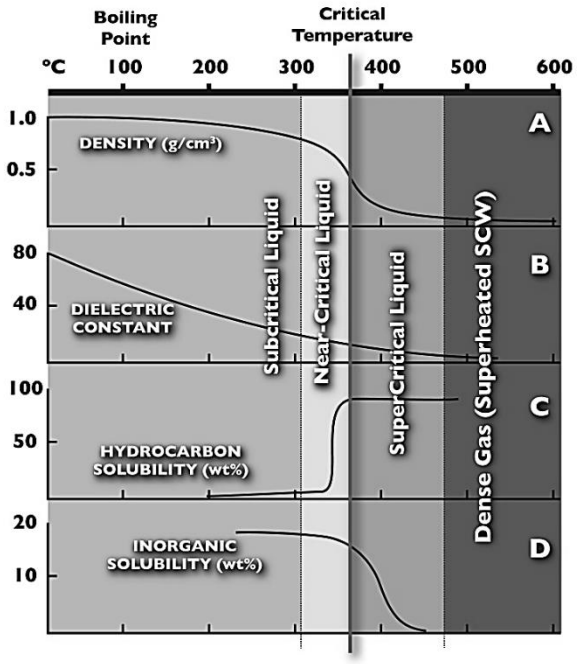

Fig. 4. Properties of water in different temperatures (Yakaboylu *et al.* 2013)

Feedstock concentration was varied from 0.83 to 2.5 wt.%, and reactor temperature was varied from 400 to 440 °C (to avoid reactor pressures more than 260 bars). The residence time was varied from 10 to 30 min to obtain the best operational conditions for non-catalytic conversion of IRS in SCW media. The carbon gasification efficiency (CGE), which is the ratio of the amount of carbon in the gas phase products to the amount of carbon in the feedstock, was calculated by following equation:

$$CGE\ (\%) = \left(\frac{\text{Carbon in Gas Phase}}{\text{Carbon in Feedstock}}\right) \times 100 \quad (9)$$

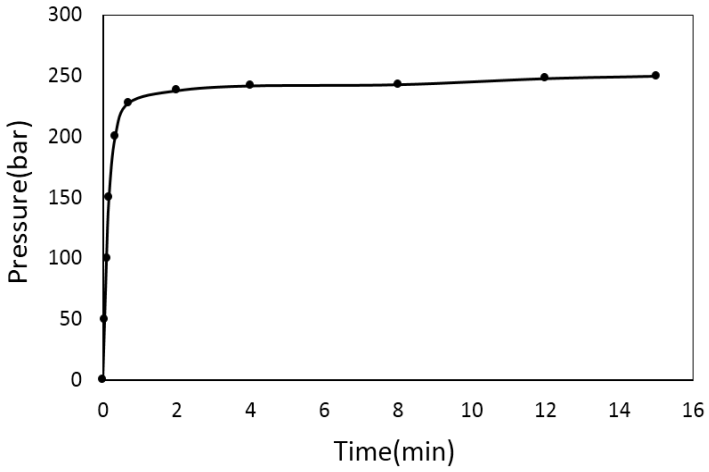

Fig. 5. A typical variation of reactor pressure with time

RESULTS AND DISCUSSION

Structural and elemental analysis of IRS

Lignocellulosic materials (*e.g.*, IRS) usually consist of carbon, oxygen, hydrogen, and trace amounts of sulfur and nitrogen. As its name implies, this feedstock contains lignin, cellulose, and hemicellulose. An elemental analysis of feedstock was done *via* a CHNS analyzer (Table 1). The oxygen content was calculated by Eq. 10:

$$O\% = 100 - C\% - H\% - N\% - S\% - Ash \quad (10)$$

The structural analysis is summarized in Table 2. This lignocellulosic feedstock has a great deal of cellulose and hemicellulose, which makes it attractive for gasification in supercritical water media to generate gaseous products.

Table 1. Elemental Analysis of IRS

Element	%
C	49.7
H	5.88
N	1.1
S	0.06
O	40.6
Ash	2.66

Table 2. Structural Analysis of IRS

Component	Wt.%
Cellulose	37.8
Hemicellulose	25.3
Lignin	28.3

Effect of temperature on supercritical water gasification of IRS

Temperature has significant impact on the gasification of biomass. Figure 6 shows the effect of temperature on SCWG of IRS. Conversion of biomass into gaseous products can be summarized in its reaction with water vapor (steam reforming). This reaction is endothermic, which makes increasing temperature desirable for feedstock decomposition.

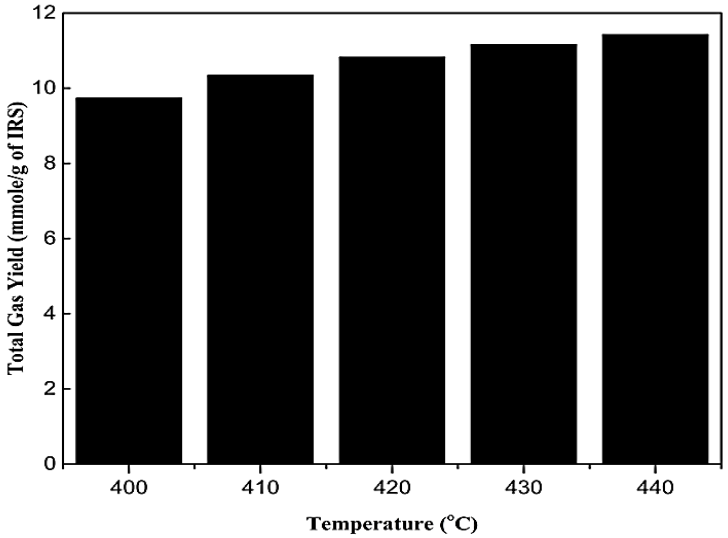

Fig. 6. The total gas production with variation of temperature (*t* = 20 min, feed concentration = 2.5 wt. %, feed loading = 0.15 g)

Based on the thermodynamics of the process, the total gas yield must be enhanced by increasing temperature. This hypothesis was confirmed in Fig. 6. Increasing the temperature from 400 to 440 °C increased the total gas yield by a factor of 1.17.

Figure 7 shows the effect of temperature on the selectivity of gaseous products. As the temperature rose from 400 to 440 °C, the H_2, CO_2, and CO production increased, while CH_4 production slightly decreased.

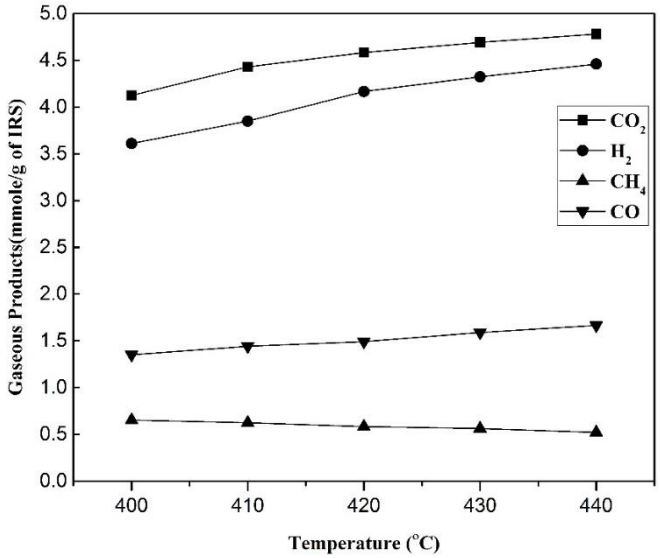

Fig. 7. Gaseous products variation with temperature (t = 20 min, feed concentration = 2.5 wt.%, feed loading = 0.15 g)

The results just described are explained by the thermodynamics of steam reforming and methanation reactions. Methanation is an exothermic reaction that is inhibited as temperature rises from 400 to 440 °C, but the increasing temperature enhances H_2 production due to the endothermic nature of steam reforming.

Figure 8 shows carbon gasification efficiency (CGE) with variations in temperature. When temperature varied from 400 to 440 °C, the CGE increased by a factor of 1.13, which is probably due to steam reforming reaction improvement by increasing temperature. Temperature enhances this endothermic reaction and feedstock degradation.

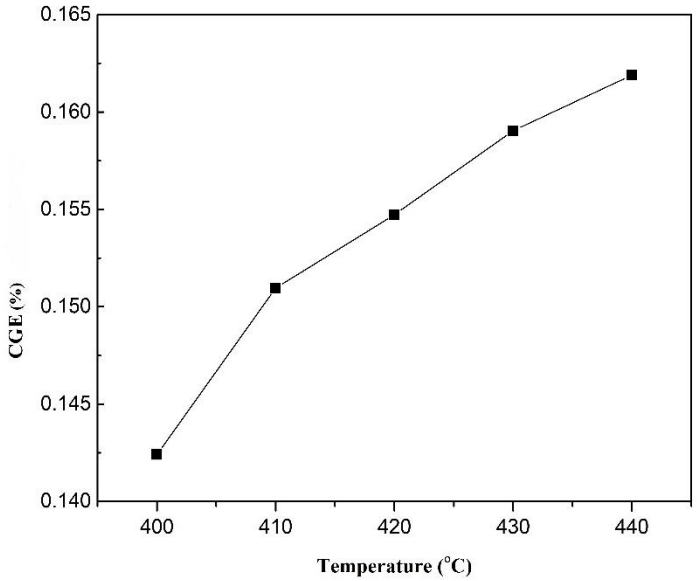

Fig. 8. Carbon gasification efficiency variation temperature (*t* = 20 min, feed concentration = 2.5 wt. %, feed loading = 0.15 g)

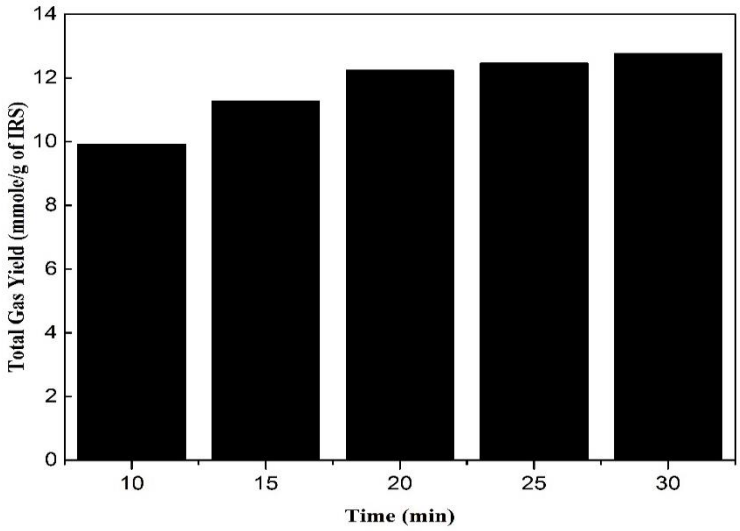

Fig. 9. Total gas yield variation with reaction time (*T*= 440 °C, feed concentration = 2.5 wt.%, feed loading = 0.15 g)

Effect of reaction time on supercritical water gasification of IRS

Figure 9 demonstrates the variation in total gas yield with reaction time. As reaction time was increased from 10 to 20 min, total gas production increased by a factor of 1.23; after that, no significant change was observed.

Due to considerable changes in total gas yield until 20 min, it can be concluded that from 10 to 20 min, the lignin content was degraded, and cellulose and hemicellulose in the biomass became accessible for better gasification. After this critical time, no significant change in gas production occurred.

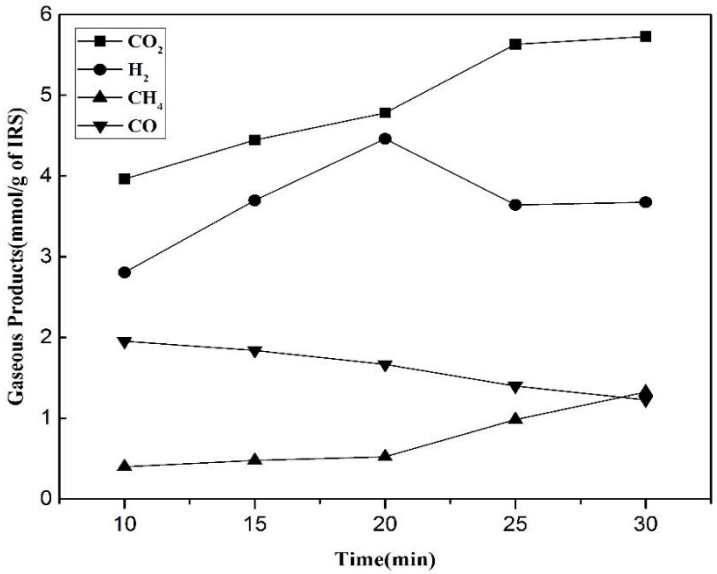

Fig. 10. Gaseous product variations versus reaction time (T= 440 °C, feed concentration = 2.5 wt.%)

Gaseous product variations *versus* reaction time are plotted in Fig. 10. As reaction time was changed from 10 to 20 min, there was a significant increase in CO_2, H_2, and CH_4 yields, while the CO yield decreased. After 20 min, H_2 decreased considerably, indicating that from 10 to 20 min, steam reforming and water-gas shift reactions were dominant to produce CO_2 and H_2 as the main gaseous components. Thereafter, methanation prevailed, and the produced H_2 was consumed for methane generation. As a result, the CO decreasing trend is due to both water-gas shift and methanation reactions, which consume CO for hydrogen and methane generation, respectively.

As shown in Fig. 11, carbon gasification efficiency varied slightly with changes in reaction time from 10 to 20 min. After that, an adverse change was observed in CGE until 25 min.

Steam reforming of feedstock resulted in mediocre carbon gasification until 20 min, but from 20 to 25 min, steam reforming and methanation reactions were dominant. Thus, carbon gasification efficiency increased drastically.

Total carbon distribution in the gas phase, liquid effluent, and solid residue were analyzed to calculate the carbon balance. Carbon balance for each experiment was calculated based on the weight percentage of converted carbon (Behnia 2013).

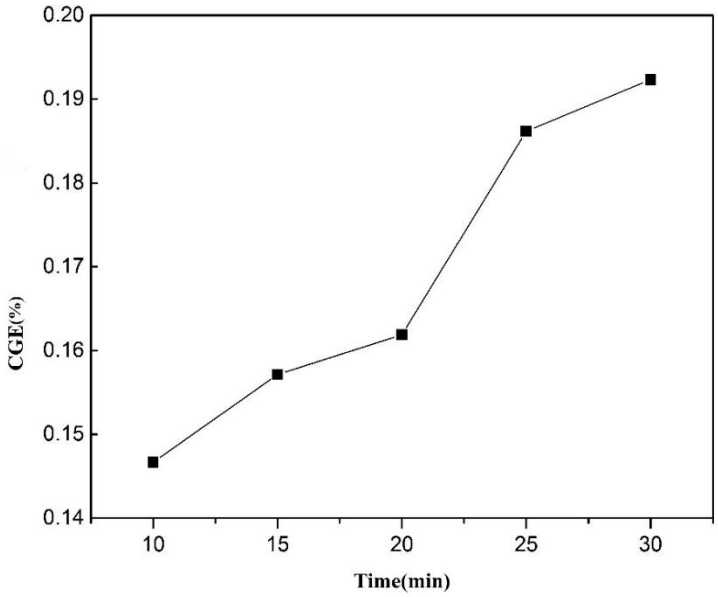

Fig. 11. Carbon gasification efficiency variations by reaction time (*T*= 440 °C, Feed Concentration = 2.5 wt. %)

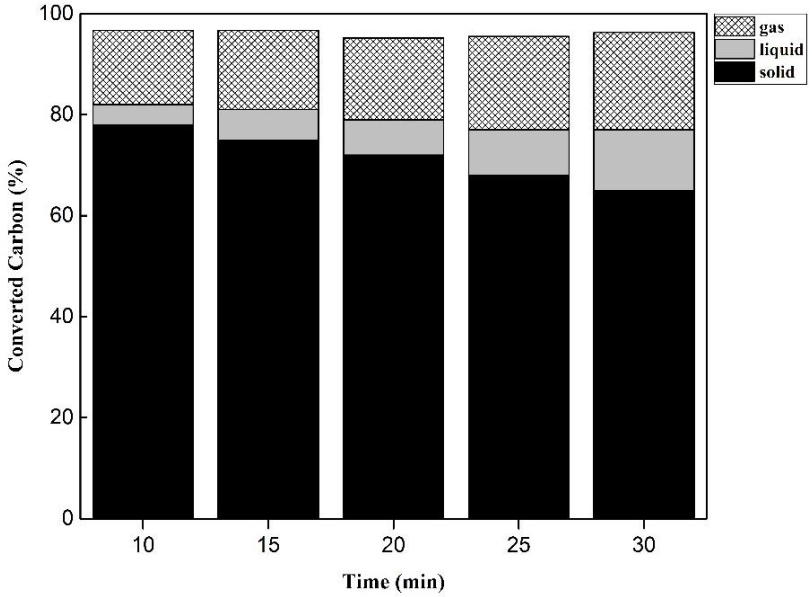

Fig. 12. weight percentage of converted carbon in gaseous, aqueous and solid phase products variation by reaction time (*T*: 440 °C, feed concentration= 2.5 wt. %)

Figure 12 depicts the weight percentage of converted carbon among gaseous, aqueous, and solid phase products. This figure also shows that as reaction time was increased from 10 to 30, the quantity of converted carbon in gaseous phase was enhanced while the amount of this parameter in two other phases began to decrease. This phenomenon could be due to better gasification efficiency at higher reaction time. The variation of carbon in the balance (from 100%) may be because of the hydrocarbons sticking to the wall of the reactor.

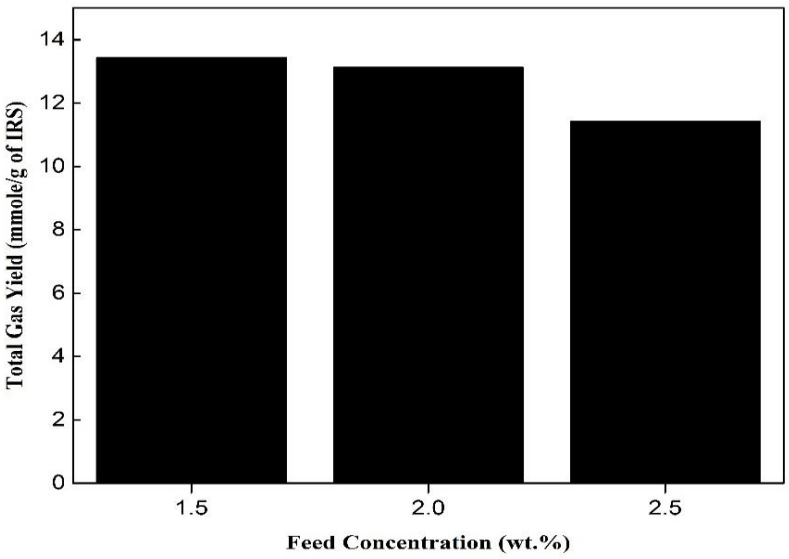

Fig. 13. Total gas production at different feed concentrations (*T* = 440 °C, *t* = 20 min)

Effect of feed concentration on supercritical water gasification of IRS

As feed concentration was varied from 1.5 to 2.5 wt.%, the total gas production decreased by a factor of 0.85 (Fig. 13). Variation of feed concentration changed the amount of available water molecules around feedstock components, which this decreased amount of water molecules impress the feed hydrolyze. Therefore, higher feed concentration decreased water molecules around feed particles, which reduced steam reforming activity in gas production.

Gaseous products variations with feed concentration are summarized in Fig. 14. H_2 and CO yield decreased when feed concentration changed from 1.5 to 2.5 wt.%, while methane generation was enhanced. The methanation reaction consumes H_2 and CO for CH_4 generation.

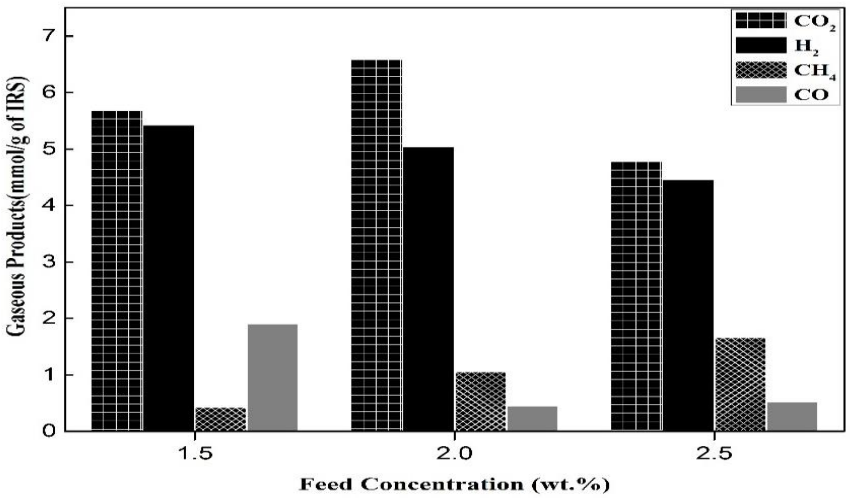

Fig. 14. Gaseous product variations versus feed concentration (*T* = 440 °C, *t* = 20 min)

Figure 15 illustrates carbon gasification efficiency at different feed concentrations. In accordance with total gas production, CGE decreased with increasing feed concentration.

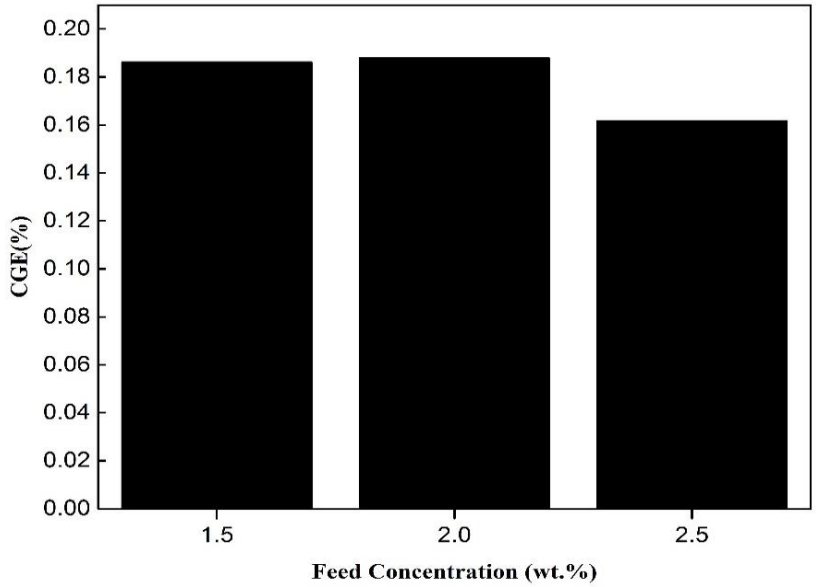

Fig. 15. CGE variations versus feed concentration (*T* = 440 °C, *t* = 20 min)

Comparison with previous results

In order to discern the difference between IRS and other agricultural wastes performance in SCW media, the current results were compared to those of an earlier study by the authors (Safari *et al.* 2015). Table 3 shows hydrogen production data which had originated from walnut shell, almond shell, wheat straw (Safari *et al*. 2015), and IRS gasification in hydrothermal media.

All of these data contributed to gasification of aforementioned feed stocks at their optimized condition. As seen in this table, wheat straw had the highest H_2 generation among these lignocellulosic materials, and other feed stocks were according to the following rating sequence:

Wheat straw > IRS > walnut shell > almond shell

Table 3. Hydrogen Production Data from Different Sources

Feed stock	Composition analysis (cellulose / hemicellulose / lignin)(Wt. %)	H_2 Generation (mmol/g of feed)	Operational condition
Wheat Straw	39.8 / 27.3 / 19.3	7.25	440˚C, 10 min, 1 wt.%
IRS	37.8 / 25.3 / 28.3	5.56	440˚C, 20 min, 2 wt.%
Walnut Shell	36 / 25.43 / 38	4.63	440˚C, 15 min, 1 wt.%
Almond Shell	30.7 / 32.6 / 35	4.1	440˚C, 20 min, 1 wt.%

As can be easily seen in the above table, an increase in lignin content from wheat straw to almond shell leads to a decrease in H_2 generation. This probably is due to lignin firm structure which leads to lower gasification of feedstock. Also it has been reported

(Yoshida and Matsumura 2001) that unsaturated structures within lignin may consume H_2 to become saturated.

CONCLUSIONS

1. The parameters of temperature, reaction time, and feed concentration were monitored as the main process variables affecting the SCWG of IRS. Of these parameters, temperature had the greatest effect. Bio-sin gas containing H_2, CO_2, CO, and CH_4 was generated by the hydrothermal gasification of Iranian rice straw, whereby CO_2 and H_2 were dominant.
2. As discussed above, higher temperature (440 °C), an intermediate value of feed concentration (2 wt.%), and reaction time (20 min) are desired for H_2 production through SCWG of IRS.
3. Since the main aim of this paper was optimization of IRS gasification in SCW media, it was shown that syn gas production is maximized at a temperature of 440 °C, reaction time of 20 min, and feed concentration equal to 2 wt. %.

REFERENCES CITED

Anon, (2014). Definition of Renewable Energy. Available at: http://www.treia.org/ renewable-energy-defined/.

Barati, M. Babatabar, M. Tavasoli, A., Dalai, A. K., and Das, U. (2014). "Hydrogen production via supercritical water gasification of bagasse using unpromoted and zinc promoted Ru/γ-Al_2O_3 nanocatalysts," *Fuel Processing Technology*, 123, 140–148. DOI: 10.1016 /j.fuproc.2014.02.005

Behnia, I. (2013). *Treatment of Aqueous Biomass and Waste via Supercritical Water Gasification for the Production of CH_4 and H_2,* Electronic Thesis and Dissertation Repository, Master of Engineering Science, University of Western Ontario, Canada.

Bridgewater, A. V. (2004). "Biomass fast pyrolysis," *Thermal Science*, 8(2), 21–50. DOI: 10.2298/TSCI0402021B

Hao, X. (2003). "Hydrogen production from glucose used as a model compound of biomass gasified in supercritical water," *International Journal of Hydrogen Energy*, 28(1), 55–64. DOI: 10.1016/S0360-3199(02)00056-3

Hiremath, R. B. Kumar, B. Balachandra, P., Ravindranath, N. H., and Raghunandan, B. N. (2009). "Decentralised renewable energy: Scope, relevance and applications in the Indian context," *Energy for Sustainable Development*, 13(1), 4-10. DOI: 10.1016 / j.esd .2008.12.001

Huang, H.-J. and Ramaswamy, S. (2011). "Thermodynamic analysis of black liquor steam gasification," *BioResources*, 6(3), 3210–3230. DOI: 10.15376/biores.6.3.3210-3230

Huber, G. W. and Dumesic, J. A. (2006). "An overview of aqueous-phase catalytic processes for production of hydrogen and alkanes in a biorefinery," *Catalysis Today*, 111(1-2), 119–132. DOI: 10.1016/j.cattod.2005.10.010

Jacobs-Young, C. J., Venditti, R. A., and Joyce, T. W. (1998). "Effect of enzymatic pretreatment on the diffusion of sodium hydroxide in wood," *Tappi Journal*, 81(1),

260–266.

Kean, C. W., Sahu, J. N. and Daud, W. M. A. W. (2013). "Hydrothermal gasification of palm shell biomass for synthesis of hydrogen fuel," *BioResources*, 8(2), 1831–1840. DOI: 10.15376/biores.8.2.1831-1840

Mehrani, R. Barati, M., Tavasoli, A., and Karimi, A. (2015). "Hydrogen production *via* supercritical water gasification of bagasse using Ni-Cu/γ-Al_2O_3 nano-catalysts," *Environmental Technology*, 36(10), 1265–72. DOI: 10.1080/09593330.2014.984771

Mohan, D., Pittman, C. U. and Steele, P. H. (2006). "Pyrolysis of wood/biomass for bio-oil: A critical review," *Energy & Fuels*, 20(3), 848–889. DOI: 10.1021/ef0502397

Rashidi, M. and Tavasoli, A. (2014). "Hydrogen rich gas production *via* noncatalytic gasification of sugar cane bagasse in supercritical water media," *Petroleum & Coal*, 56(3), 324–331.

Safari, F. Tavasoli, A. Ataei, A. and Choi, J. K. (2015). "Non-catalytic conversion of wheat straw, walnut shell and almond shell into hydrogen rich gas in supercritical water media," *Chinese Journal of Chemical Engineering*. 4(2), 121–125.

Susanti, R. F., Dianningrum, L. W., Yum, T., Kim, Y., Gwon Lee, B., and Kim, J. (2012). "High-yield hydrogen production from glucose by supercritical water gasification without added catalyst," *International Journal of Hydrogen Energy*, 37(16), 11677–11690. DOI: 10.1016/j.ijhydene.2012.05.087

Tavasoli, A., Barati, M. and Karimi, A. (2015). "Sugarcane bagasse supercritical water gasification in presence of potassium promoted copper nano-catalysts supported on γ-Al_2O_3," *International Journal of Hydrogen Energy*, 41(1), 174-180. DOI: 10.1016/j.ijhydene.2015.09.026

Tekin, K., Karagöz, and S. Bektaş, S. (2014). "A review of hydrothermal biomass processing," *Renewable and Sustainable Energy Reviews*, 40, 673–687. DOI: 10.1016/j.rser.2014.07.216

Yakaboylu, O., Harinck, J., Gerton Smit, K. G., and De Jong, W. (2013). "Supercritical water gasification of manure: A thermodynamic equilibrium modeling approach," *Biomass and Bioenergy*, 59, 253–263. DOI: 10.1016/j.biombioe.2013.07.011

Yoshida, T., and Matsumura, Y. (2001). "Gasification of cellulose, xylan, and lignin mixtures in supercritical water," *Industrial & Engineering Chemistry Research*, 40(23), 5469–5474. DOI: 10.1021/ie0101590

Yu, H., Yang, X., Jiang, L., and Chen, D. (2014). "Experimental study on co-gasification characteristics of biomass and plastic wastes." *BioResources*, 9(3), 5615–5626. DOI: 10.15376/biores.9.3.5615-5626

Article submitted: March 3, 2016; Peer review completed: May 9, 2016; Revised version received: May 18, 2016; Accepted: May 20, 2016; Published: June 13, 2016.
DOI: 10.15376/biores.11.3.6362-6377